yeast Pol II are homologous to RPC1 and RPC2 of Pol III, respectively. Asn620_Lys652 in RPC2 corresponds to Tyr679_Lys712 in RPB2. The deletion of Asn620_Lys652 (Tyr679_Lys712) would destroy a structural core of RPB2, leading to loss of RPB2 function. In addition, Arg768 (Arg852 in RPB2) interacts with the main-chain carbonyl group of Arg70 of the RPB12 subunit, and Asp926 (Asp1009 in RPB2) interacts with the side chain of Arg48 of the RPB10 subunit of Pol II (Figure 1D). Arg768His (Arg852His) and Asp926Glu (Asp1009Glu) substitutions are considered to disturb these subunit interactions, leading to dysfunction of the polymerase. Therefore, structural prediction suggests that the mutations in *POLR3B* (RPC2) could affect Pol III function. On the other hand, Ile897 and Arg1005 in RPC1 correspond to Val863 and Arg1036 in RPB1, respectively. Ile897 (Val863) has hydrophobic interactions with Leu170 and Pro176 of the RPB5 subunit and with Phe900 (Phe866) of the RPB1 subunit of Pol II (Figure 1E). Ile897Asn (Val863Asn) substitution is likely to disturb this interaction. Arg1005 (Arg1036) stabilizes interaction between RPB1 and RPB8 subunits (Figure 1F). The Arg1005Cys (Arg1036Cys) substitution appears to make this interaction unstable. Thus mutations in *POLR3A* are also predicted to affect Pol III function.

Clinical features of individuals with *POLR3A* or *POLR3B* mutations are presented in Table 1. MRI revealed high-intensity areas in the white matter in T2-weighted images, cerebellar atrophy, and a hypoplastic corpus callosum in all four individuals (Figure 3). Individuals 1 and 2 showed an extremely similar clinical course. They developed normally during their early infancy, i.e., walking unaided at 15 and 14 months, and uttering a few words at 12 and 13 months, respectively. After the age of 3, individual 1 presented with unstable walking and frequent stumbling and falling down, and individual 2 became poor at exercise. They both had severe myopia (corrected visual acuity of 0.7 and 0.5 at most, respectively). They graduated from elementary, junior high, and high schools with poor records, and the intelligence quotient (IQ) of individual 2 was 52 (WAIS-III). In individual 1, unstable walking was prominent at around 18 years, and he could not ride a bicycle because of ataxia; however, he could drive an automobile. Amenorrhea was noted in individual 2, and was successfully treated by hormone therapy. Individual 1 showed several signs of hypogonadism, including absence of underarm and mustache hair, thin pubic hair (Tanner II), and serum levels of testosterone, follicle stimulating hormone, and luteinizing hormone that were below normal for age 27. Neurological examination of both individuals revealed mild horizontal nystagmus, slowing of smooth-pursuit eye movement, and gaze limitation, especially in vertical gazing, hypotonia, mildly exaggerated deep-tendon reflex (patellar and Achilles tendon reflex) with negative Babinski reflex, and cerebellar signs and symptoms, including ataxic speech, wide-based ataxic gait, dysdiadochokinesis, and dysmetria. Clinical information for individual 3 has been reported previously.[6] Additional findings are as follows: slowing of smooth-pursuit eye movement, gaze limitation in vertical gazing, normal auditory brain responses (ABR), cerebral symptoms with mild spasticity, and intellectual disability (an IQ of 43 according to the WISC-III test), and no myopia but hypermetropic astigmatism. She showed no deterioration besides a mild dysphagia and walks herself to a school for the disabled. Individual 4 developed normally during his

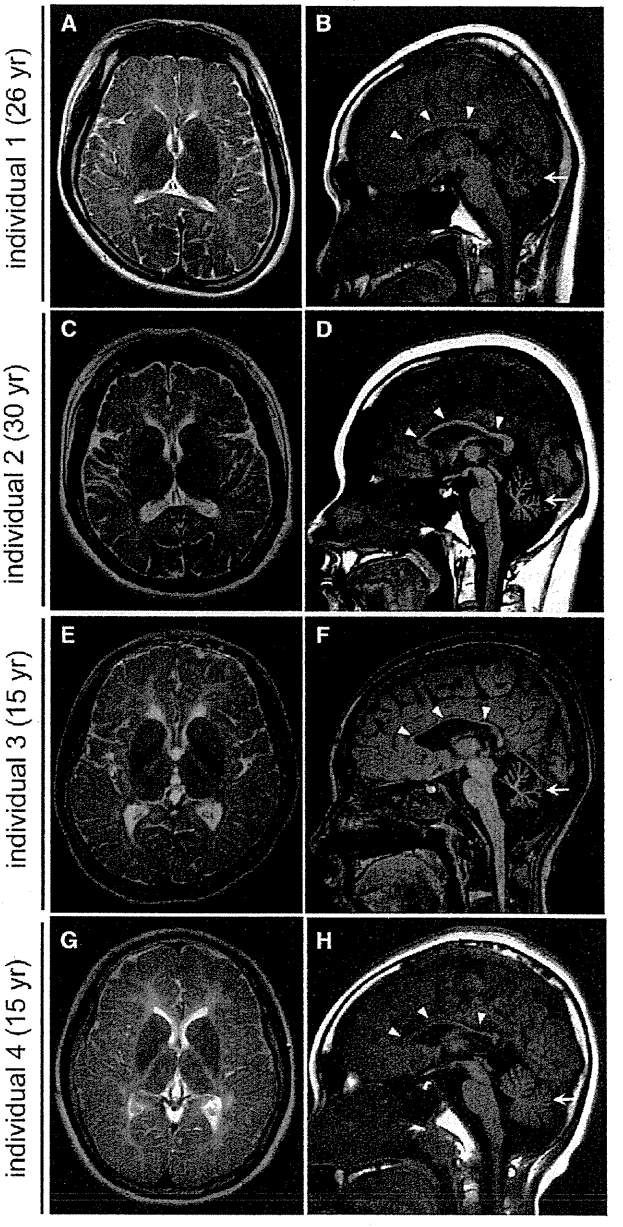

Figure 3. Brain MRI of Individuals with *POLR3B* and *POLR3A* Mutations

(A, C, E, and G) T2-weighted axial images through the basal ganglia. High-intensity areas in the white matter were observed in all individuals.

(B, D, F, and H) T1-weighted midline sagittal images. All the individuals showed hypoplastic corpus callosum (arrowheads) and atrophy of cerebellum (arrows).

early infancy, had normal head control at 3 months, was speaking a few words at 12 months, and was walking unaided at 14 months. His parents noted mild tremors around 4 years. He had normal stature, weight, and head circumference. Although he had severe myopia, his eye movement was smooth with no limitation or nystagmus. He had sensory neuronal deafness on the left side. He showed normal muscle tone and had no spasticity or rigidity. His tendon reflexes were slightly elevated with a negative Babinski reflex. Cerebellar signs were noted; expressive ataxic explosive speech, intension tremor, poor finger to nose test, dysdiadochokinesis, dysmetria, and wide-based ataxic gait. His intelligence quotient was 57 (according to the WISC-III test). His peripheral nerve conduction velocity was within the normal range and his ABR showed normal responses on the right side. He suffered motor deterioration around age 14 and became wheelchair bound.

In this study, we successfully identified compound heterozygous mutations in *POLR3A* and *POLR3B* in individuals with HCAHC. Very recently, Bernard et al.[12] reported that *POLR3A* mutations cause three overlapping leukodystrophies, including 4H syndrome, suggesting that HCAHC is, at least in part, within a wide clinical spectrum caused by *POLR3A* mutations. The p.Arg1005Cys mutation was shared between individual 9 in their report and our individual 4. All 19 individuals with *POLR3A* mutations showed progressive upper motor neuron dysfunction and cognitive regression. In addition, individual 9 showed abnormal eye movement, hypodontia, and hypogonadism. None of these features were recognized in our individual 4; these differences further support phenotypic variability of *POLR3A* mutations.[12] Given the phenotypic similarities among 4H syndrome, HCAHC, and H-ABC, there is a possibility that H-ABC is also allelic and caused by recessive mutations in either *POLR3A* or *POLR3B*.

Pol III consists of 17 subunits and is involved in the transcription of small noncoding RNAs, such as 5S ribosomal RNA (rRNA), U6 small nuclear RNA (snRNA), 7SL RNA, RNase P, RNase MRP, short interspersed nuclear elements (SINEs), and all transfer RNAs (tRNAs). Pol III-transcribed genes are classified into three types based on promoter elements and transcription factors. 5S rRNA is a solo type I gene. Type II genes include tRNA, 7SL RNA, and SINEs. Type III genes include U6 snRNA, RNase P, and RNase MRP.[18–20] The Pol III system is important for cell growth in yeast, and its transcription is tightly regulated during the cell cycle.[20] In zebrafish, *polr3b* mutant larvae that have a deletion of 41 conserved amino acids (Δ239-279) from the Rpc2 protein showed a proliferation deficit in multiple tissues, including intestine, endocrine pancreas, liver, retina and terminal branchial arches.[21] In the mutants, the expression levels of tRNA were significantly reduced, whereas the level of 5S rRNA expression was not changed, suggesting that this *polr3b* mutation can differentially affect Pol III target promoters.[21] RPC2 contributes to the catalytic activity of the polymerase and forms the active center of the polymerase together with the largest subunit, RPC1.[22] Thus, it is reasonable to consider that mutations in *POLR3A* and *POLR3B* cause overlapping phenotypes. Indeed, three individuals with *POLR3B* mutations showed diffuse cerebral hypomyelination, atrophy of the cerebellum and corpus callosum, and abnormal eye movements that overlap with *POLR3A* abnormalities.[12] Furthermore, two out of three individuals showed hypogonadism, suggesting a common pathological mechanism between *POLR3A* and *POLR3B* mutations. In the zebrafish *polr3b* mutants there were no defects of the central nervous system other than a reduced size of the retina, probably reflecting species differences; however, the reduced level of tRNA in the *polr3b* mutants raises the possibility that defects of tRNA transcription by Pol III could be a common pathological mechanism underlying *POLR3A* and *POLR3B* mutations. Supporting this idea, mutations in two genes involved in aminoacylation activity of tRNA synthetase cause defects of myelination in central nervous system: *DARS2* (MIM 610956) and *AIMP* (MIM 603605).[23,24] In addition, mutations in four genes encoding aminoacyl-tRNA synthetase cause Charcot-Marie-Tooth disease (MIM 613641, 613287, 601472, and 608323), resulting from demyelination of peripheral nerve axons: *KARS* (MIM 601421), *GARS* (MIM 600287), *YARS* (MIM 603623), and *AARS* (MIM 601065).[25–28] Thus, it is very likely that regulation of tRNA expression is essential for development and maintenance of myelination in both central and peripheral nervous systems.

An interesting clinical feature of *POLR3B* mutations is the absence of motor deterioration. All three individuals with *POLR3B* mutations could walk without support at ages 16, 27, and 30, whereas individual 3 with *POLR3A* mutations had motor deterioration around age 14. Bernard et al.[12] also reported progressive upper motor neuron dysfunction and cognitive regression in individuals with *POLR3A* mutations. Thus, there is a possibility that phenotypes caused by *POLR3A* mutations could be more severe and progressive than *POLR3B* mutant phenotypes. Identification of a greater number of cases with *POLR3B* mutations is required to confirm this hypothesis.

In conclusion, our data, together with that of a previous report,[12] demonstrate that mutations in Pol III subunits cause overlapping autosomal-recessive hypomyelinating disorders. Establishment of an animal model will facilitate our understanding of the pathophysiology of the multiple defects caused by Pol III mutations.

Supplemental Data

Supplemental Data include three tables and can be found with this article online at http://www.cell.com/AJHG/.

Acknowledgments

We would like to thank all the individuals and their families for their participation in this study. This work was supported by

research grants from the Ministry of Health, Labour, and Welfare (H.S., H.O., M.S., J.T., N. Miyake, K.I. and N. Matsumoto), the Japan Science and Technology Agency (N. Matsumoto), a Grant-in-Aid for Scientific Research on Innovative Areas (Foundation of Synapse and Neurocircuit Pathology) from the Ministry of Education, Culture, Sports, Science and Technology of Japan (N. Matsumoto), a Grant-in-Aid for Scientific Research from Japan Society for the Promotion of Science (H.O., N. Matsumoto), a Grant-in-Aid for Young Scientist from Japan Society for the Promotion of Science (H.S.). This work has been done at Advanced Medical Research Center, Yokohama City University.

Received: August 31, 2011
Revised: October 5, 2011
Accepted: October 10, 2011
Published online: October 27, 2011

Web Resources

The URLs for data presented herein are as follows:

ClustalW, http://www.genome.jp/tools/clustalw/
dbSNP, http://www.ncbi.nlm.nih.gov/projects/SNP/
Ensembl, http://uswest.ensembl.org/index.html
GenBank, http://www.ncbi.nlm.nih.gov/Genbank/
Online Mendelian Inheritance in Man, http://www.omim.org
PolyPhen-2, http://genetics.bwh.harvard.edu/pph2/
Protein Data Bank, http://www.pdb.org/pdb/home/home.do
PyMOL, http://www.pymol.org/
SeattleSeq Annotation, http://gvs.gs.washington.edu/SeattleSeqAnnotation/

References

1. Schiffmann, R., and van der Knaap, M.S. (2009). Invited article: an MRI-based approach to the diagnosis of white matter disorders. Neurology *72*, 750–759.
2. Timmons, M., Tsokos, M., Asab, M.A., Seminara, S.B., Zirzow, G.C., Kaneski, C.R., Heiss, J.D., van der Knaap, M.S., Vanier, M.T., Schiffmann, R., and Wong, K. (2006). Peripheral and central hypomyelination with hypogonadotropic hypogonadism and hypodontia. Neurology *67*, 2066–2069.
3. Wolf, N.I., Harting, I., Boltshauser, E., Wiegand, G., Koch, M.J., Schmitt-Mechelke, T., Martin, E., Zschocke, J., Uhlenberg, B., Hoffmann, G.F., et al. (2005). Leukoencephalopathy with ataxia, hypodontia, and hypomyelination. Neurology *64*, 1461–1464.
4. Wolf, N.I., Harting, I., Innes, A.M., Patzer, S., Zeitler, P., Schneider, A., Wolff, A., Baier, K., Zschocke, J., Ebinger, F., et al. (2007). Ataxia, delayed dentition and hypomyelination: a novel leukoencephalopathy. Neuropediatrics *38*, 64–70.
5. van der Knaap, M.S., Naidu, S., Pouwels, P.J., Bonavita, S., van Coster, R., Lagae, L., Sperner, J., Surtees, R., Schiffmann, R., and Valk, J. (2002). New syndrome characterized by hypomyelination with atrophy of the basal ganglia and cerebellum. AJNR Am. J. Neuroradiol. *23*, 1466–1474.
6. Sasaki, M., Takanashi, J., Tada, H., Sakuma, H., Furushima, W., and Sato, N. (2009). Diffuse cerebral hypomyelination with cerebellar atrophy and hypoplasia of the corpus callosum. Brain Dev. *31*, 582–587.
7. Li, H., Ruan, J., and Durbin, R. (2008). Mapping short DNA sequencing reads and calling variants using mapping quality scores. Genome Res. *18*, 1851–1858.
8. Doi, H., Yoshida, K., Yasuda, T., Fukuda, M., Fukuda, Y., Morita, H., Ikeda, S., Kato, R., Tsurusaki, Y., Miyake, N., et al. (2011). Exome sequencing reveals a homozygous *SYT14* mutation in adult-onset, autosomal-recessive spinocerebellar ataxia with psychomotor retardation. Am. J. Hum. Genet. *89*, 320–327.
9. Pierce, S.B., Walsh, T., Chisholm, K.M., Lee, M.K., Thornton, A.M., Fiumara, A., Opitz, J.M., Levy-Lahad, E., Klevit, R.E., and King, M.C. (2010). Mutations in the DBP-deficiency protein HSD17B4 cause ovarian dysgenesis, hearing loss, and ataxia of Perrault Syndrome. Am. J. Hum. Genet. *87*, 282–288.
10. Gilissen, C., Arts, H.H., Hoischen, A., Spruijt, L., Mans, D.A., Arts, P., van Lier, B., Steehouwer, M., van Reeuwijk, J., Kant, S.G., et al. (2010). Exome sequencing identifies *WDR35* variants involved in Sensenbrenner syndrome. Am. J. Hum. Genet. *87*, 418–423.
11. Saitsu, H., Kato, M., Okada, I., Orii, K.E., Higuchi, T., Hoshino, H., Kubota, M., Arai, H., Tagawa, T., Kimura, S., et al. (2010). *STXBP1* mutations in early infantile epileptic encephalopathy with suppression-burst pattern. Epilepsia *51*, 2397–2405.
12. Bernard, G., Chouery, E., Putorti, M.L., Tetreault, M., Takanohashi, A., Carosso, G., Clement, I., Boespflug-Tanguy, O., Rodriguez, D., Delague, V., et al. (2011). Mutations of *POLR3A* Encoding a Catalytic Subunit of RNA Polymerase Pol III Cause a Recessive Hypomyelinating Leukodystrophy. Am. J. Hum. Genet. *89*, 415–423.
13. Jasiak, A.J., Armache, K.J., Martens, B., Jansen, R.P., and Cramer, P. (2006). Structural biology of RNA polymerase III: subcomplex C17/25 X-ray structure and 11 subunit enzyme model. Mol. Cell *23*, 71–81.
14. Fernández-Tornero, C., Böttcher, B., Riva, M., Carles, C., Steuerwald, U., Ruigrok, R.W., Sentenac, A., Müller, C.W., and Schoehn, G. (2007). Insights into transcription initiation and termination from the electron microscopy structure of yeast RNA polymerase III. Mol. Cell *25*, 813–823.
15. Cramer, P., Bushnell, D.A., and Kornberg, R.D. (2001). Structural basis of transcription: RNA polymerase II at 2.8 angstrom resolution. Science *292*, 1863–1876.
16. Gnatt, A.L., Cramer, P., Fu, J., Bushnell, D.A., and Kornberg, R.D. (2001). Structural basis of transcription: an RNA polymerase II elongation complex at 3.3 A resolution. Science *292*, 1876–1882.
17. Wang, D., Bushnell, D.A., Huang, X., Westover, K.D., Levitt, M., and Kornberg, R.D. (2009). Structural basis of transcription: backtracked RNA polymerase II at 3.4 angstrom resolution. Science *324*, 1203–1206.
18. Oler, A.J., Alla, R.K., Roberts, D.N., Wong, A., Hollenhorst, P.C., Chandler, K.J., Cassiday, P.A., Nelson, C.A., Hagedorn, C.H., Graves, B.J., and Cairns, B.R. (2010). Human RNA polymerase III transcriptomes and relationships to Pol II promoter chromatin and enhancer-binding factors. Nat. Struct. Mol. Biol. *17*, 620–628.
19. Dieci, G., Fiorino, G., Castelnuovo, M., Teichmann, M., and Pagano, A. (2007). The expanding RNA polymerase III transcriptome. Trends Genet. *23*, 614–622.
20. Dumay-Odelot, H., Durrieu-Gaillard, S., Da Silva, D., Roeder, R.G., and Teichmann, M. (2010). Cell growth- and differentiation-dependent regulation of RNA polymerase III transcription. Cell Cycle *9*, 3687–3699.

21. Yee, N.S., Gong, W., Huang, Y., Lorent, K., Dolan, A.C., Maraia, R.J., and Pack, M. (2007). Mutation of RNA Pol III subunit *rpc2/polr3b* Leads to Deficiency of Subunit Rpc11 and disrupts zebrafish digestive development. PLoS Biol. *5*, e312.
22. Werner, M., Thuriaux, P., and Soutourina, J. (2009). Structure-function analysis of RNA polymerases I and III. Curr. Opin. Struct. Biol. *19*, 740–745.
23. Scheper, G.C., van der Klok, T., van Andel, R.J., van Berkel, C.G., Sissler, M., Smet, J., Muravina, T.I., Serkov, S.V., Uziel, G., Bugiani, M., et al. (2007). Mitochondrial aspartyl-tRNA synthetase deficiency causes leukoencephalopathy with brain stem and spinal cord involvement and lactate elevation. Nat. Genet. *39*, 534–539.
24. Feinstein, M., Markus, B., Noyman, I., Shalev, H., Flusser, H., Shelef, I., Liani-Leibson, K., Shorer, Z., Cohen, I., Khateeb, S., et al. (2010). Pelizaeus-Merzbacher-like disease caused by AIMP1/p43 homozygous mutation. Am. J. Hum. Genet. *87*, 820–828.
25. Latour, P., Thauvin-Robinet, C., Baudelet-Méry, C., Soichot, P., Cusin, V., Faivre, L., Locatelli, M.C., Mayençon, M., Sarcey, A., Broussolle, E., et al. (2010). A major determinant for binding and aminoacylation of tRNA(Ala) in cytoplasmic Alanyl-tRNA synthetase is mutated in dominant axonal Charcot-Marie-Tooth disease. Am. J. Hum. Genet. *86*, 77–82.
26. McLaughlin, H.M., Sakaguchi, R., Liu, C., Igarashi, T., Pehlivan, D., Chu, K., Iyer, R., Cruz, P., Cherukuri, P.F., Hansen, N.F., et al. (2010). Compound heterozygosity for loss-of-function lysyl-tRNA synthetase mutations in a patient with peripheral neuropathy. Am. J. Hum. Genet. *87*, 560–566.
27. Antonellis, A., Ellsworth, R.E., Sambuughin, N., Puls, I., Abel, A., Lee-Lin, S.Q., Jordanova, A., Kremensky, I., Christodoulou, K., Middleton, L.T., et al. (2003). Glycyl tRNA synthetase mutations in Charcot-Marie-Tooth disease type 2D and distal spinal muscular atrophy type V. Am. J. Hum. Genet. *72*, 1293–1299.
28. Jordanova, A., Irobi, J., Thomas, F.P., Van Dijck, P., Meerschaert, K., Dewil, M., Dierick, I., Jacobs, A., De Vriendt, E., Guergueltcheva, V., et al. (2006). Disrupted function and axonal distribution of mutant tyrosyl-tRNA synthetase in dominant intermediate Charcot-Marie-Tooth neuropathy. Nat. Genet. *38*, 197–202.

CLINICAL GENETICS An International Journal of Genetics, Molecular and Personalized Medicine

Clin Genet 2011: 80: 293–296
Printed in Singapore. All rights reserved

CLINICAL GENETICS
doi: 10.1111/j.1399-0004.2011.01644.x

Letter to the Editor

A novel homozygous mutation of *DARS2* may cause a severe LBSL variant

To the Editor:

Leukoencephalopathy with brain stem and spinal cord involvement, and lactate elevation (LBSL, MIM #611105) is an autosomal recessive disorder with an early childhood-to-adolescence onset. In 2003, van der Knaap et al. originally described LBSL, which is characterized by slowly progressive pyramidal, cerebellar, and dorsal column dysfunction with increased white matter lactate levels in magnetic resonance (MR) spectroscopy (1). Since the first discovery that LBSL is caused by mutations of the *DARS2* gene-encoding mitochondrial aspartyl-tRNA synthetase (MtAspRS) (2), *DARS2* mutations have been found in all the patients described (2–5), but none of them showed a homozygous mutation (all are compound heterozygotes), suggesting that the activity of mutant MtAspRS homodimers may be incompatible with human life (2, 5). Here, we describe, for the first time, a consanguineous family with a homozygous *DARS2* mutation.

Materials and methods

We analyzed a consanguineous family including three affected children diagnosed with leukoencephalopathy (Fig. 1a and Table 1). The proband (II-2) developed truncal ataxic gait at 3 years old. Her affected sister (II-3) and brother (II-4) also showed truncal ataxia at 6 and 11 months, respectively. All cases were presented with horizontal nystagmus, slurring speech, ataxic gait, muscle tonus abnormality, hypo- or hyperreflexia, and tremor as well as mental retardation. II-2 at age 21 years could slowly speak one or two words. Peripheral muscles atrophy, weakness and joints contractures in extremities, loss of deep tendons reflex and disturbed deep sensation were noted. II-3 and II-4 died of pneumonia at age 8 years and respiratory failure at age 2 years, respectively. Although there were differences in MR imaging characteristics from classical LBSL, there were also striking similarities. In our patients, the involvement of the cerebral and cerebellar white matter was more diffused and severe than in classical LBSL, but the affected brain stem and spinal cord tracts were the same (Fig. 1b and Table 1).

Linkage analysis and direct sequencing of *DARS2* were performed as previously reported (6). Immunoblotting was carried out using antihuman DARS2 antibody (ab69336, Abcam, Cambridge, UK) and anti-cytochrome *c* oxidase (COX) IV antibody (ab16056, Abcam).

Results

Homozygosity mapping of this consanguineous family revealed the largest 8.5 Mb homozygous region at chromosome 1q25.1 with the maximum LOD score of 1.329. Five additional microsatellite markers showed the consistent result (Fig. 1a). Within this region, *DARS2* gene was highlighted as the primary target as it was causative for the LBSL. We found that all affected children possessed homozygous, and parents and an unaffected sib had the heterozygous intronic change at 22 base pairs upstream of exon 3 (c.228-22T>A), respectively. This change was not observed in 395 controls. We examined its mutational effect by reverse transcriptase-polymerase chain reaction (RT-PCR) using mRNA of lymphoblastoid cell lines (LCLs) derived from the proband, her father (a carrier) and a normal control. A shorter PCR fragment which lacked the entire exon 3 was confirmed by sequencing (Fig. 1c,d). Furthermore, wild-type *DARS2* mRNA and MtAspRS protein were significantly decreased in proband's LCL (Fig. 1e,f). Other genes within the 1q25.1 region have not been checked.

Discussion

We found a novel homozygous mutation of *DARS2* in a diffuse leukoencephalopathy, which may be an LBSL variant. This change resulted in the decrease of normal protein level and may have contributed to this disease. Two possibilities for the increased severity are considered: (i) a

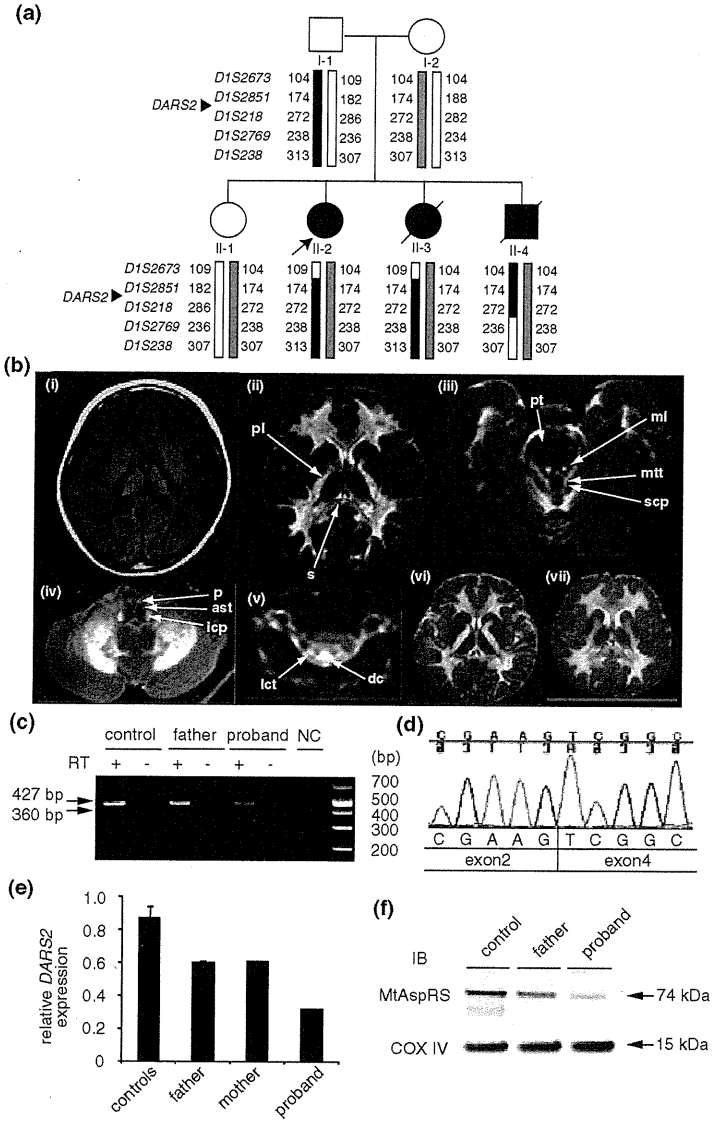

Fig. 1. Identification of a homozygous *DARS2* mutation causing abnormal splicing. (**a**) Haplotype analysis of the family. The black and gray bars represent disease alleles. The *DARS2* gene is located in between *D1S2851* and *D1S218*. (**b**) Magnetic resonance (MR) images of central nervous system in the proband (II-2) at 5 years (i–v), II-3 at 5 years (vi) and II-4 at 1 year and 4 months of age (vii). T_1-weighted (i) and T_2-weighted (T_2) (ii) images of cerebrum. The cerebral white matter was diffusely and severely affected, while the cerebral white matter involvement is less severe and more limited in extent in leukoencephalopathy with brain stem and spinal cord involvement, and lactate elevation with sparing of the U-fibers. Inhomogeneous signal abnormalities were observed in the posterior limb (pl) of the internal capsule and the splenium (s) of the corpus callosum. (iii) T_2 image at the level of the pons. The abnormal high-intensity signals were observed in pyramidal tracts (pt), medial lemniscus (ml), mesencephalic trigeminal tracts (mtt) and superior cerebellar peduncles (scp). (iv) T_2 image at the level of medulla. The pyramids (p), anterior spinocerebellar tracts (ast) and inferior cerebellar peduncles (icp) were affected. (v) T_2 image at the level of the cervical spinal cord. The dorsal columns (dc) and lateral corticospinal tracts (lct) showed abnormal signals. II-3 (vi) and II-4 (vii) showed the similar MR images as the proband. (**c**) RT-PCR using cDNA extracted from LCLs of a normal control, father and the proband. A shorter fragment (360 bp) in addition to a normal product (427 bp) was seen in father and the proband. (**d**) Electropherogram of the shorter fragment showing skipping of exon 3. (**e**) Relative expression of wild-type *DARS2* mRNA compared to β-actin mRNA in LCLs were determined by quantitative real-time RT-PCR using TaqMan Gene Expression Assays (Applied Biosystems, Bedford, MA). The relative *DARS2* expression was analyzed using TaqMan Probe (Applied Biosystems, Hs01016215_m1 for *DARS2* and 4326135E for β-actin as a control). Levels are shown for three controls, parents and the proband based on the calibration curve method using an independent control. Average of duplicated experiments is shown as black bars with the standard error of means. The significant decreased expression of *DARS2* mRNA in the proband was recognized compared to that in three controls ($p < 0.001$, one-way analysis of variance with Bonferroni's multiple comparison test). (**f**) Mitochondrial aspartyl-tRNA synthetase (MtAspRS) protein is expressed in normal control and father as a carrier (fainter), but only weakly recognized in the proband. Cyclooxygenase IV was used as a loading control for the mitochondrial fraction.

Table 1. MRI criteria for LBSL and clinical features of patients

Diagnostic criteria	Case 1	Case 2	Case 3
Major criteria			
Signal abnormalities in			
1. the cerebral white matter, either inhomogeneous and spotty or homogeneous and confluent, sparing the U-fibers	±[a]	±[a]	±[a]
2. the dorsal columns and lateral corticospinal tracts of the spinal cord. (visualization of such abnormalities in the cervical spinal cord suffices)	+	n.e.[b]	n.e.
3. the pyramids of the medulla oblongata	+	+	+
Supportive criteria			
Signal abnormalities in			
1. the splenium of the corpus callosum	+	+	+
2. the posterior limb of the internal capsule	+	+	+
3. the medial lemniscus in the brain stem	+	+	+
4. the superior cerebellar peduncles	+	+	+
5. the inferior cerebellar peduncles	+	n.e.	n.e.
6. the intraparenchymal part of the trigeminal nerve	−	n.e.	n.e.
7. the mesencephalic trigeminal tracts	+	n.e.	n.e.
8. the anterior spinocerebellar tracts in the medulla	+	n.e.	n.e.
9. the cerebellar white matter with subcortical preponderance	−	−	−
Elevated lactate of abnormal cerebral white matter (MRS)	+	Not performed	+

LBSL, leukoencephalopathy with brain stem and spinal cord involvement, and lactate elevation; MRI, magnetic resonance imaging; MRS, magnetic resonance spectroscopy.
[a]Homogeneous and confluent abnormal high intensity was observed, but sparing the U-fibers was unclear because of the strenuous pathological change in the white matter.
[b]n.e., not evaluated as MRI images were unavailable.

(unidentified) modifier effect in the family and (ii) this particular homozygous mutation caused the severe variant because of the substantially decreased normal protein level, although it is not full proof.

Interestingly, affected allele frequency varies, depending on the ethnicity. For example, *DARS2* mutations are the most common causes of childhood onset leukoencephalopathy in Finland, because of high carrier frequency (1:95 for the c.228-20_21delTTinsC and 1:380 for the c.492+2T>C) (4). Thus, further analysis of the *DARS2* gene in LBSL as well as childhood-to-adult onset leukoencephalopathy of unknown cause in different populations would lead us to fully understand phenotypes of the *DARS2* abnormalities.

Acknowledgements

We thank all the patients and their families for participating in this work. We also thank Ms. Y. Yamashita for her technical assistance. This work was supported by Research Grants from the Ministry of Health, Labour and Welfare (N. M., H. S., and N. M.), the Japan Science and Technology Agency (N. M.), Grant-in-Aid for Scientific Research from Japan Society for the Promotion of Science (N. M.), Grant-in-Aid for Young Scientist from Japan Society for the Promotion of Science (N. M. and H. S.), Grant for 2010 Strategic Research Promotion of Yokohama City University (N. M.), Research Grants from the Japan Epilepsy Research Foundation (H. S.), and Research Grant from Naito Foundation (N. M.), the Takeda Science Foundation (N. M. and N. M.), the Yokohama Foundation for Advancement of Medical Science (N. M.), and the Hayashi Memorial Foundation for Female Natural Scientists (N. M.).

N Miyake[a]
S Yamashita[b]
K Kurosawa[c]
S Miyatake[a]
Y Tsurusaki[a]
H Doi[a]
H Saitsu[a]
N Matsumoto[a]
[a]Department of Human Genetics, Yokohama City University Graduate School of Medicine, Yokohama, Japan,
[b]Division of Child Neurology, and
[c]Division of Medical Genetics, Kanagawa Children's Medical Center, Yokohama, Japan

References

1. van der Knaap MS, van der Voorn P, Barkhof F et al. A new leukoencephalopathy with brainstem and spinal cord involvement and high lactate. Ann Neurol 2003: 53: 252–258.
2. Scheper GC, van der Klok T, van Andel RJ et al. Mitochondrial aspartyl-tRNA synthetase deficiency causes leukoencephalopathy with brain stem and spinal cord involvement and lactate elevation. Nat Genet 2007: 39: 534–539.
3. Uluc K, Baskan O, Yildirim KA et al. Leukoencephalopathy with brain stem and spinal cord involvement and high lactate:

a genetically proven case with distinct MRI findings. J Neurol Sci 2008: 273: 118–122.
4. Isohanni P, Linnankivi T, Buzkova J et al. *DARS2* mutations in mitochondrial leucoencephalopathy and multiple sclerosis. J Med Genet 2010: 47: 66–70.
5. Lin J, Faria EC, Da Rocha AJ et al. Leukoencephalopathy with brainstem and spinal cord involvement and normal lactate: a new mutation in the *DARS2* gene. J Child Neurol 2010: 25: 1425–1428.
6. Miyake N, Kosho T, Mizumoto S et al. Loss-of-function mutations of *CHST14* in a new type of Ehlers-Danlos syndrome. Hum Mutat 2010: 31: 966–974.

Correspondence:
Noriko Miyake, MD, PhD
Department of Human Genetics
Yokohama City University Graduate School of Medicine
3-9 Fukuura
Kanazawa-ku
236-0004 Yokohama
Japan
Tel.: +81 45 787 2606
Fax: +81 45 786 5219
e-mail: nmiyake@yokohama-cu.ac.jp

CLINICAL REPORT

AMERICAN JOURNAL OF medical genetics PART A

Early Infantile Epileptic Encephalopathy Associated With the Disrupted Gene Encoding Slit-Robo Rho GTPase Activating Protein 2 (*SRGAP2*)

Hirotomo Saitsu,[1]* Hitoshi Osaka,[2] Shirou Sugiyama,[2] Kenji Kurosawa,[3] Takeshi Mizuguchi,[1] Kiyomi Nishiyama,[1] Akira Nishimura,[1] Yoshinori Tsurusaki,[1] Hiroshi Doi,[1] Noriko Miyake,[1] Naoki Harada,[4] Mitsuhiro Kato,[5] and Naomichi Matsumoto[1]

[1]Department of Human Genetics, Graduate School of Medicine, Yokohama City University, Kanazawa-ku, Yokohama, Japan

[2]Division of Neurology, Clinical Research Institute, Kanagawa Children's Medical Center, Minami-ku, Yokohama, Japan

[3]Division of Medical Genetics, Clinical Research Institute, Kanagawa Children's Medical Center, Minami-ku, Yokohama, Japan

[4]Cytogenetic Testing Group B, Advanced Medical Science Research Center, Mitsubishi Chemical Medience Corporation, Nagasaki, Japan

[5]Faculty of Medicine, Department of Pediatrics, Yamagata University Yamagata, Japan

Received 25 January 2011; Accepted 31 July 2011

We report on a female patient with early infantile epileptic encephalopathy and severe psychomotor disability possessing a de novo balanced translocation t(1;9)(q32;q13). The patient showed clonic convulsions of extremities 2 days after birth. Electroencephalogram (EEG) transiently showed atypical suppression-burst pattern. The seizures evolved to brief tonic spasms, and hypsarrhythmia on EEG was noticed at age of 5 months, indicating the transition to West syndrome. By using fluorescent in situ hybridization (FISH), southern hybridization, and inverse PCR, the translocation breakpoints were successfully determined at the nucleotide level. The 1q32.1 breakpoint was located within a segmental duplication and disrupted the gene encoding Slit-Robo Rho GTPase activating protein 2 (*SRGAP2*). The 9q13 breakpoint was suggested to reside in the heterochromatin region. *Srgap2* has been shown to be specifically expressed in developing brain of rodents, negatively regulate neuronal migration and induce neurite outgrowth and branching. Thus, *SRGAP2* is very likely to play a role in the developing human brain. This is a first report of the *SRGAP2* abnormality associated with early infantile epileptic encephalopathy.

Key words: early infantile epileptic encephalopathy; West syndrome; chromosomal translocation; *SRGAP2*

How to Cite this Article:
Saitsu H, Osaka H, Sugiyama S, Kurosawa K, Mizuguchi T, Nishiyama K, Nishimura A, Tsurusaki Y, Doi H, Miyake N, Harada N, Kato M, Matsumoto N. 2012. Early infantile epileptic encephalopathy associated with the disrupted gene encoding Slit-Robo Rho GTPase activating protein 2 (*SRGAP2*).
Am J Med Genet Part A 158A:199–205.

INTRODUCTION

Many infantile epileptic syndromes show a unique combination of seizure types and electroencephalogram (EEG) findings depending on the patients' age [Kato et al., 2008]. Ohtahara syndrome (OS) and early myoclonic encephalopathy (EME) are characterized by early onset seizures mainly in neonatal period, and suppression-burst pattern on EEG, though their initial seizure type is different [Djukic et al., 2006; Ohtahara and Yamatogi, 2006]. Both OS and EME can progress to the West syndrome phenotype age-dependently, which is characterized by brief tonic spasms, a specific EEG pattern called hypsarrhythmia [Kato, 2006], in 75% and 41% of cases, respectively [Djukic et al., 2006; Ohtahara and Yamatogi, 2006]. The three epileptic syndromes (OS, EME, and West syndrome) are generally intractable and show the arrest of psychomotor development [Djukic et al., 2006; Kato, 2006; Ohtahara and Yamatogi, 2006]. Brain malformations and metabolic disorders were found as underlying causes of the three syndromes, but

Grant sponsor: Ministry of Health, Labour and Welfare; Grant sponsor: Japan Society for the Promotion of Science; Grant sponsor: Yokohama Foundation for Advancement of Medical Science; Grant sponsor: Japan Epilepsy Research Foundation; Grant sponsor: Naito Foundation.

*Correspondence to:
Dr. Hirotomo Saitsu, Department of Human Genetics, Yokohama City University Graduate School of Medicine, Fukuura 3-9, Kanazawa-ku, Yokohama 236-0004, Japan. E-mail: hsaitsu@yokohama-cu.ac.jp

Published online 21 November 2011 in Wiley Online Library (wileyonlinelibrary.com).
DOI 10.1002/ajmg.a.34363

many idiopathic or cryptogenic cases remain etiologically unexplained. Recently, several causative genes have been reported: *ARX* in OS and West syndrome, *CDKL5* in West syndrome, *STXBP1* in OS, *SLC25A22* in EME [Stromme et al., 2002; Kalscheuer et al., 2003; Weaving et al., 2004; Molinari et al., 2005; Kato et al., 2007; Saitsu et al., 2008]. Of note, mutations in *ARX* have been found in both OS and West syndrome phenotypes, suggesting a common pathological seizure mechanism between them. However, there are still large numbers of cases remaining to be elucidated. Identification of new causative genes is absolutely necessary for further understanding of infantile epileptic syndromes.

The Slit-Robo signaling controls the neuronal migration and axonal guidance [Brose et al., 1999; Li et al., 1999; Wu et al., 1999], both of which are dependent on cytoskeletal reorganization. The family of Rho-GTPases, including Rac, Cdc42, and Rho, plays important roles in regulating cytoskeletal dynamics [Hall, 1998]. Rho-GTPases alternate between active (GTP-bound) and inactive (GDP-bound) conformation. The activities of Rho GTPases are tightly and antagonistically regulated by Guanine nucleotide exchange factors (GEFs) and GTPase activating proteins (GAPs): GEFs catalyze nucleotide exchange and mediate activation, while GAPs increase the intrinsic GTPase activities to promote GTP hydrolysis, leading to inactivation [Lamarche and Hall, 1994]. Slit-Robo Rho GTPase activating proteins (SRGAPs) were identified as a family of GAP proteins which bind to the intracellular domain of Robo [Wong et al., 2001]. Three family members (SRGAP1-3) specifically expressed in developing brain of rodents [Wong et al., 2001; Yao et al., 2008; Bacon et al., 2009]. Recent studies suggested that SRGAPs are involved in neuronal development. SRGAP1 protein is required for Slit-mediated repulsion of migratory cells from the anterior subventricular zone of the forebrain by blocking Cdc42 activity [Wong et al., 2001]. Functional disruption of SRGAP3 protein is associated with severe mental retardation in 3p-syndrome [Endris et al., 2002]. Moreover, it has been reported that SRGAP2 negatively regulates neuronal migration and induces neurite outgrowth and branching [Guerrier et al., 2009].

Here, we present a patient with infantile epileptic encephalopathy and profound psychomotor delay with a de novo reciprocal translocation t(1;9)(q32;q13), disrupting the *SRGAP2* gene. Detailed genomic analysis is presented.

CLINICAL REPORT

The 5-year-old girl is a product of unrelated healthy parents. She was born at term without asphyxia after an uneventful pregnancy. She showed apnea twice at day 1. Clonic convulsions of extremities started at day 2. Initial EEG performed at 10-day was reported as normal. Subsequently, myoclonus, which was easily induced by stimulation, was observed. Ictal EEG during myoclonus did not indicate that it was an electronical convulsion. Clonic convulsions were increased at 2 months of age when atypical suppression-burst pattern was transiently observed (Fig. 1A). Her seizures were controlled by combination of vitamin B6, zonisamide, phenobarbital, and KBr, but myoclonus continued. Brain magnetic resonance imaging (MRI) showed cortical atrophy and thin corpus callosum at 2 months of age (Fig. 1C–E). West syndrome was diagnosed at 5 months of age by intellectual disability without head control, series of tonic-spasms, and hypsarrhysmia on EEG (Fig. 1B).

MATERIALS AND METHODS

Molecular Cytogenetic Analysis

G-banded chromosomes of peripheral lymphocytes were analyzed. Fluorescence in situ hybridization (FISH) was performed using peripheral lymphocytes. Labeling, hybridization, wash, and image acquisition were performed as previously described [Saitsu et al., 2008]. RPCI-11 BAC clones and approximately 10-kb probes amplified by long PCR using LA Taq polymerase (Takara Bio, Otsu, Japan) were used as probes. Primer information is available on request.

GeneChip Human Mapping 250K *Nsp*I Array

Genomic DNA obtained from peripheral blood leukocytes were used for microarray analysis. Experimental procedures were performed according to the manufacturer's protocol with slight modification (fragmentation time was shortened to 25 min). Call rate was 89.5%. Copy number alterations were analyzed by using CNAG2.0 [Nannya et al., 2005].

Cloning of Translocation Breakpoints

The 1q32.1 translocation breakpoint was analyzed by Southern hybridization using *Eco*RI- and *Pst*I-digested patient DNA. Her parental DNAs were also analyzed. Probes were synthesized by PCR DIG probe synthesis kit (Roche, Basel, Switzerland) using RP11-134f21 DNA as a template. Primer information is available on request. Hybridization, washing and detection of probes were done according to the manufacturer's protocol. Images were captured on FluorChem (Alpha Innotech, San Leandro, CA). After identification of aberrant DNA fragments by Southern hybridization, size fractioning of electrophoresed *Eco*RI- and *Pst*I-digested DNA of the patient was performed using QIAEXII Gel extraction kit (Qiagen, Valencia, CA) in order to obtain der(1) and der(9) translocation junction fragments, respectively. The collected DNA was self-ligated by Ligation high (Toyobo, Osaka, Japan), ethanol precipitated and dissolved in 20 μl EB buffer (Qiagen). Inverse PCR was performed in 25 μl of volume, containing 2 μl ligated DNA, 1× LA PCR bufferII, 2.5 mM $MgCl_2$, 0.4 mM each dNTP, 0.5 μM each primer, and 1.25 U LA Taq polymerase (Takara Bio). Primers were listed below: *Eco*RI-forward, 5′-GAAATGGCCTGGCTTGGTTGCTAT-3′; *Eco*RI-reverse, 5′-CACTGAAGCTGCCCTTGAGAAGTGA-3′; *Pst*I-forward, 5′-TTTCCCTCCATGATTCCTCTCTGCT-3′; *Pst*I-reverse, 5′-CCAGGACAGCGTCTCACTCTCCATA-3′. Negative controls only used either forward or reverse primer. The PCR product was purified with ExoSAP (USB Co., Cleveland, OH) and sequenced for both forward and reverse strands with BigDye Terminator chemistry ver. 3 according to the standard protocol (Applied Biosystems, Foster city, CA). After breakpoint sequences were determined, breakpoint-specific primers for both der(1) and der(9) translocation junctions were designed: der(1)-forward, 5′-CCAAGGAATTGGGATCTCTGGGTCT -3′; der(1)-reverse, 5′-CATTCCATTCCATTCCCCTGCAC -3′ (1,098-bp);

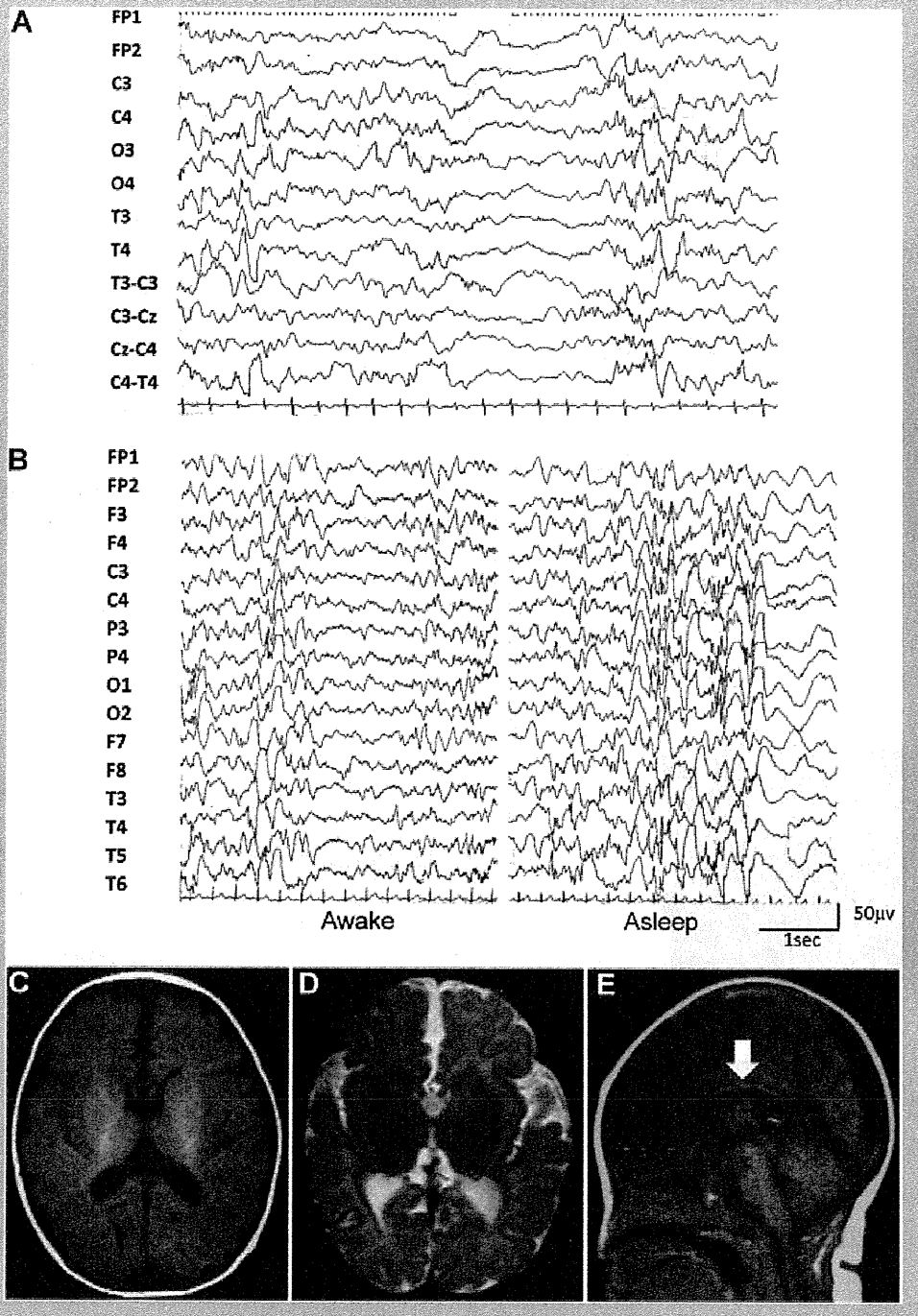

FIG. 1. EEG and brain MRI of the patient. A: Interictal high-voltage bursts alternate with low amplitude suppression phases at an approximately regular rate in both awake and asleep states at age of 2 months. Suppression phases do not exhibit "almost flat pattern" as typical suppression-burst pattern. B: Interictal EEG at 5 months shows multifocal spikes at awake (left), and high-voltage slow rhythm superimposed with irregular spikes; hypsarrhythmia at sleep with some periodicity (right). C,D: Brain MRI T1- (C) and T2-weighted (D) axial images show mild cortical atrophy with normal myelination. E: Sagital brain T1-weighted image shows thin corpus callosum (arrow)

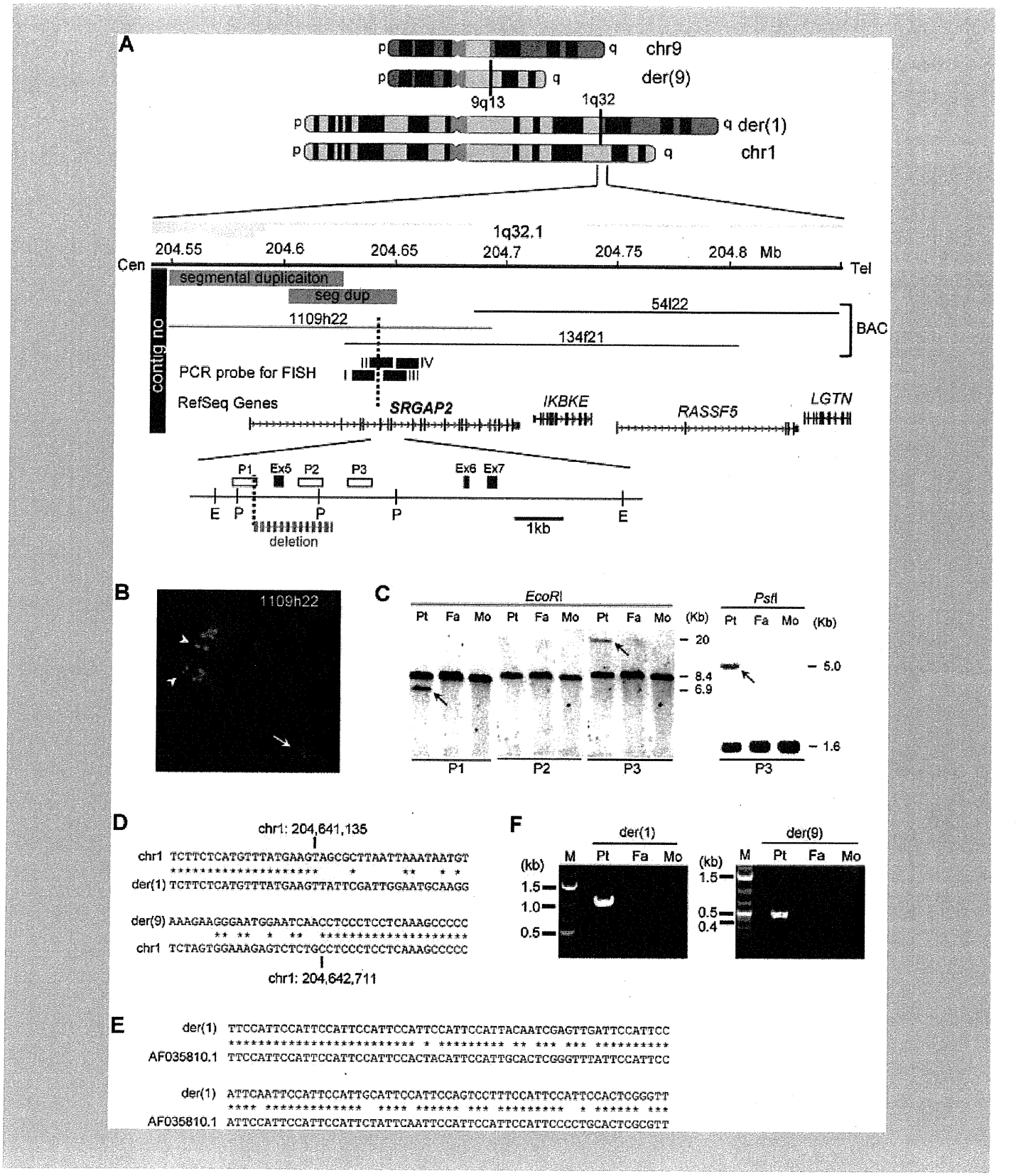
A
chr9
der(9)
der(1)
chr1
9q13
1q32
1q32.1
204.55
204.6
204.65
204.7
204.75
204.8 Mb
Cen
Tel
segmental duplicaiton
seg dup
contig no
1109h22
54l22
134f21
BAC
PCR probe for FISH
RefSeq Genes
SRGAP2
IKBKE
RASSF5
LGTN
P1
Ex5
P2
P3
Ex6
Ex7
E
P
1kb
deletion
B
1109h22
C
EcoRI
PstI
Pt
Fa
Mo
(Kb)
20
8.4
6.9
5.0
1.6
P1
P2
P3
D
chr1: 204,641,135
chr1 TCTTCTCATGTTTATGAAGTAGCGCTTAATTAAATAATGT
der(1) TCTTCTCATGTTTATGAAGTTATTCGATTGGAATGCAAGG
der(9) AAAGAAGGGAATGGAATCAACCTCCCTCCTCAAAGCCCCC
chr1 TCTAGTGGAAAGAGTCTCTGCCTCCCTCCTCAAAGCCCCC
chr1: 204,642,711
F
der(1)
der(9)
M
(kb)
1.5
1.0
0.5
0.4
E
der(1) TTCCATTCCATTCCATTCCATTCCATTCCATTACAATCGAGTTGATTCCATTCC
AF035810.1 TTCCATTCCATTCCATTCCATTCCACTACATTCCATTGCACTCGGGTTTATTCCATTCC
der(1) ATTCAATTCCATTCCATTGCATTCCATTCCAGTCCTTTCCATTCCATTCCACTCGGGTT
AF035810.1 ATTCCATTCCATTCCATTCTATTCAATTCCATTCCATTCCATTCCCCTGCACTCGCGTT

der(9)-forward, 5′-GGAAAGGAATGGAATGAAATCAACGCG-3′; der(9)-reverse, 5′-CCAGGACAGCGTCTCACTCTCCATA-3′ (495-bp). Junction fragments were amplified by PCR using these primer-sets on DNAs of the patient and her parents.

RESULTS

G-banded chromosomal analysis revealed a balanced translocation t(1;9)(q32;q13). Her parents showed a normal karyotype (data not shown), indicating that the translocation occurred de novo. Subsequent FISH analysis demonstrated that the breakpoint in chromosome 1 was covered by the clones, RP11-1109h22 and 134f21, showing signals all on normal chromosome 1 and derivatives chromosomes 1 and 9 (Fig. 2A,B). The overlapping region of these two clones was localized within the *SRGAP2* locus (Fig. 2A). The 5′-part of *SRGAP2* transcript was not mapped in the Human Genome browser (both in NCBI Build 36.1/hg18 and GRCh37/hg19 assembly) because the genomic contigs covering the immediately upstream regions of *SRGAP2* gene were absent. Thus, we described the putative exon number based on the order of mappable exons to the existing genomic database. The breakpoint was further narrowed down by FISH analysis using long PCR products as probes (Fig. 2A). Probe II showed weak but clear signals all in on chromosome 1, and derivative chromosomes 1 and 9, suggesting that the breakpoint was located within probe II (data not shown). It was of note that the probe II is associated with a segmental duplication (Fig. 2A). Southern hybridization analysis using probes P1 and P3 detected different aberrant bands only in the patient (Fig. 2A,C), indicating that the 1q32 breakpoint was located at the region between the two probes. P2 did not show any aberrant bands in Southern analysis, suggesting that a small deletion may have occurred near the breakpoint (Fig. 2A,C). Inverse PCR [Triglia et al., 1988] on *Eco*RI- and *Pst*I-digested DNA was successful in obtaining der(1) and der(9) breakpoint-junction fragments, respectively. Sequence analysis showed that the 1q32 translocation breakpoint was located within the putative intron 5 of *SRGAP2*, and exon 5 was completely deleted (Fig. 2A). Sequences of the 9q13 breakpoint were not uniquely mapped to reference sequences. However, sequences of 3′-end of the der(1) junction fragment (approximately 6.1-kb apart from the breakpoint) were similar to satellite 3 sequences (GeneBank accession number AF035810.1) (Fig. 2E), suggesting that 9q13 breakpoint was located in the heterochromatin region. Breakpoint-specific PCR analysis of the patient and her parents confirmed that the rearrangements occurred de novo (Fig. 2F). To check genomic copy number alterations accompanied by the rearrangement, GeneChip Human Mapping 250K *Nsp*I (Affymetrix, Santa Clara, CA) was performed. Besides two known copy number variations, no other imbalances were detected (data not shown).

DISCUSSION

SRGAP2 is a member of Slit-Robo Rho GTPase activating proteins with three domains: an N-terminal F-BAR domain, a RhoGAP domain, and an SH3 domain [Wong et al., 2001; Guerrier et al., 2009]. There are three variants of *SRGAP2* transcripts in humans: variant 1 (GenBank accession number NM_015326.2), variant 2 (GenBank accession number NM_001042758.1), and variant 3 (GenBank accession number NM_001170637.1). In all three variants, the coding proteins commonly possess F-BAR, RhoGAP, and SH3 domains except for an amino acid deletion in F-BAR domain in variant 2. Mouse *Srgap2* is expressed in the entire developing cortex including proliferative zones and postmitotic regions [Bacon et al., 2009; Guerrier et al., 2009]. It has been reported that the SRGAP2 protein negatively regulates neuronal migration and induce neurite outgrowth and branching through its F-BAR domain [Guerrier et al., 2009]. In addition, GAP activity of the SRGAP2 protein specifically downregulate Rac1 [Guerrier et al., 2009]. Mutations in *ARHGEF6*, Rac1/Cdc42 specific GEF, cause X-linked mental retardation [Kutsche et al., 2000]. Moreover, mutation and/or disruption of *OPHN1* and *SRGAP3*, both encoding Rac1-GAPs, are associated with severe mental retardation [Billuart et al., 1998; Endris et al., 2002], indicating the importance of Rac1 regulation in human brain development. Thus, SRGAP2 is likely to play important roles in developing brain in humans through the ability of the F-BAR and RhoGAP domains. It would be interesting to analyze

FIG. 2. Genomic characterization of t(1;9)(q32;q13). A: Schematic representation of the reciprocal translocation, t(1;9)(q32;q13) (top). A summarized physical map covering the 1q32.1 translocation breakpoint is indicated (middle). RP11-1109h22 and 134f21, and PCR probe II span the translocation breakpoint (longitudinal dashed line) in association with the segmental duplication. Four RefSeq genes, including *SRGAP2* spanning the breakpoint, are presented. Note that absence of genomic contigs of the immediately upstream region of the *SRGAP2* gene. More detailed maps are shown (bottom). A partial restriction map (E, *Eco*RI; P, *Pst*I), probes for southern hybridization (P1–P3), and putative exons 5–7 of *SRGAP2* are indicated. Translocation breakpoint (longitudinal dashed line) accompanied with a 1,575-bp deletion encompassing exon 5 of *SRGAP2* (red thick dashed line) are located between P1 and P3. B: FISH analysis using RP11-1109h22 as a probe showed clear signals on chromosome 1, and der(1) (white arrowheads) and der(9) chromosomes (white arrow). Cross-hybridization was also observed to segmental duplications located at pericentric regions of chromosome 1 and derivative chromosome 1. C: Southern hybridization using probes P1, P2, and P3 on genomic DNAs of the patient and her parents. Arrow shows aberrant bands specific to the patient (not observed in parental DNA). Pt, patient; Fa, father; Mo, mother. D: Breakpoint junction sequences of der(1) and der(9). In upper part, top and bottom sequence strands show chromosome 1 and derivative chromosome 1 sequences, respectively. In lower part, top and bottom strands show derivative chromosome 9 and normal chromosome 1 sequences, respectively. Breakpoint positions are marked with small longitudinal lines based on the UCSC genome browser coordinate (version Mar. 2006). Asterisks indicate nucleotides identical to normal chromosomes. E: Sequences of the 3′-end of the der(1) junction fragment. Top and bottom sequence strands show der(1) and satellite 3 sequences, respectively, showing homology between two sequences. F: Breakpoint-specific PCR analysis of the patient's family. Primers specific to der(1) and der(9) breakpoints could successfully amplify 1,098- and 495-bp products, respectively, only from the patient (Pt), indicating the translocation occurred de novo. M, size marker; Fa, father; Mo, mother.

SRGAP2 in a large cohort of patients presenting with early epileptic encephalopathy including West syndrome. Although full-length *SRGAP2* transcripts (functional), which include sequences of putative exons 1–20 at 1q32.1, have been deposited in GeneBank, 5′-part of the *SRGAP2* transcript is not mapped in the Human Genome browser. Furthermore, seven exons of *SRGAP2* were again mapped to two separated segmental duplications at 1q21.1 and 1p11.2 with sequence similarities of 99.29% and 99.30%, respectively (Fig. 2A). This complex genomic structure interfered with full-blown mutation screening especially for the 1,356-bp coding region including the F-BAR domain. A microdeletion within two separate segmental duplications in *SRGAP2* locus has been found in 2 out of 90 Yoruban individuals (presumably with normal phenotype) from the HapMap Project using custom high-density oligonucleotide arrays [Matsuzaki et al., 2009]. However, it is uncertain whether they could confirm the precise locations of the deletions by another method. Thus, there remains a possibility that the deletion actually ocurred at highly homologous genomic segments located at 1q21.1 and 1p11.2. Further descriptions about aberrations of the *SRGAP2* gene will be required for establishing in a causative role in early infantile epileptic encephalopathy.

The 9q13 breakpoint is likely to reside within the heterochromatic region. It is possible that some genes adjacent to 1q32.1 breakpoint would suffer from gene silencing by the position effect. *IKBKE* is an IKK (inhibitor of nuclear factor kappaB kinase)-related kinase that is essential for interferon-inducible antiviral transcriptional response [Tenoever et al., 2007]. *Ikbke* knockout mice are protected from high-fat diet-induced obesity, chronic inflammation in liver and fat, hepatic steatosis, and whole-body insulin resistance [Chiang et al., 2009]. However, neurological abnormalities have never been reported. *RASSF5* is a member of the Ras association domain family. A crutial role in the integrin-mediated adhesion and migration of lymphocytes and dendritic cells has been shown in *Rassf5*-deficient mice, but neurological abnormalities have never been mentioned [Katagiri et al., 2004]. Thus, *IKBKE* and *RASSF5*, two adjacent genes to *SRGAP2*, are less likely to be involved in infantile epileptic encephalopathy.

In conclusion, we described a patient with early infantile epilepsitic encephalopathy, carrying a de novo reciprocal translocation disrupting the *SRGAP2* gene. Clonic convulsions and atypical suppression-burst patterns on EEG at early infantile period did not fit into either OS or EME. However, the seizures became brief tonic spasms, and hypsarrhythmia on EEG was noticed, indicating transition to West syndrome. Disruption of *SRGAP2* may be related to West syndrome which has heterogeneous backgrounds [Kato, 2006].

ACKNOWLEDGMENTS

We would like to thank the patient and her families for their participation in this study. This work was supported by Research Grants from the Ministry of Health, Labour and Welfare (H.S. and N. Matsumoto), Grant-in-Aid for Scientific Research from Japan Society for the Promotion of Science (N. Matsumoto), Grant-in-Aid for Young Scientist from Japan Society for the Promotion of Science (H.S.), Research Promotion Fund from Yokohama Foundation for Advancement of Medical Science (H.S.), Research Grants from the Japan Epilepsy Research Foundation (H.S.), and Research Grant from Naito Foundation (N. Matsumoto).

REFERENCES

Bacon C, Endris V, Rappold G. 2009. Dynamic expression of the Slit-Robo GTPase activating protein genes during development of the murine nervous system. J Comp Neurol 513:224–236.

Billuart P, Bienvenu T, Ronce N, des Portes V, Vinet MC, Zemni R, Roest Crollius H, Carrie A, Fauchereau F, Cherry M, Briault S, Hamel B, Fryns JP, Beldjord C, Kahn A, Moraine C, Chelly J. 1998. Oligophrenin-1 encodes a rhoGAP protein involved in X-linked mental retardation. Nature 392:923–926.

Brose K, Bland KS, Wang KH, Arnott D, Henzel W, Goodman CS, Tessier-Lavigne M, Kidd T. 1999. Slit proteins bind Robo receptors and have an evolutionarily conserved role in repulsive axon guidance. Cell 96:795–806.

Chiang SH, Bazuine M, Lumeng CN, Geletka LM, Mowers J, White NM, Ma JT, Zhou J, Qi N, Westcott D, Delproposto JB, Blackwell TS, Yull FE, Saltiel AR. 2009. The protein kinase IKKepsilon regulates energy balance in obese mice. Cell 138:961–975.

Djukic A, Lado FA, Shinnar S, Moshe SL. 2006. Are early myoclonic encephalopathy (EME) and the Ohtahara syndrome (EIEE) independent of each other? Epilepsy Res 70:S68–S76.

Endris V, Wogatzky B, Leimer U, Bartsch D, Zatyka M, Latif F, Maher ER, Tariverdian G, Kirsch S, Karch D, Rappold GA. 2002. The novel Rho-GTPase activating gene MEGAP/ srGAP3 has a putative role in severe mental retardation. Proc Natl Acad Sci USA 99:11754–11759.

Guerrier S, Coutinho-Budd J, Sassa T, Gresset A, Jordan NV, Chen K, Jin WL, Frost A, Polleux F. 2009. The F-BAR domain of srGAP2 induces membrane protrusions required for neuronal migration and morphogenesis. Cell 138:990–1004.

Hall A. 1998. Rho GTPases and the actin cytoskeleton. Science 279: 509–514.

Kalscheuer VM, Tao J, Donnelly A, Hollway G, Schwinger E, Kubart S, Menzel C, Hoeltzenbein M, Tommerup N, Eyre H, Harbord M, Haan E, Sutherland GR, Ropers HH, Gecz J. 2003. Disruption of the serine/ threonine kinase 9 gene causes severe X-linked infantile spasms and mental retardation. Am J Hum Genet 72:1401–1411.

Katagiri K, Ohnishi N, Kabashima K, Iyoda T, Takeda N, Shinkai Y, Inaba K, Kinashi T. 2004. Crucial functions of the Rap1 effector molecule RAPL in lymphocyte and dendritic cell trafficking. Nat Immunol 5:1045–1051.

Kato M. 2006. A new paradigm for West syndrome based on molecular and cell biology. Epilepsy Res 70:S87–S95.

Kato M, Saitoh S, Kamei A, Shiraishi H, Ueda Y, Akasaka M, Tohyama J, Akasaka N, Hayasaka K. 2007. A longer polyalanine expansion mutation in the ARX gene causes early infantile epileptic encephalopathy with suppression-burst pattern (Ohtahara syndrome). Am J Hum Genet 81: 361–366.

Kato M, Saitoh S, Kamei A, Shiraishi H, Ueda Y, Akasaka M, Tohyama J, Akasaka N, Hayasaka K., 2008. Genetic etiology of age-dependent epileptic encephalopathy in infancy: Longer polyalanine expansion in ARX causes earlier onset and more severe phenotype. In: Takahashi T, Fukuyama Y, editors. Biology of seizure susceptibility in developing brain. Montrouge, Paris: John Libbey Eurotext. pp. 75–86.

Kutsche K Yntema H Brandt A Jantke I Nothwang HG Orth U Boavida MG David D Chelly J Fryns JP Moraine C Ropers HH Hamel BC van Bokhoven H Gal A 2000 Mutations in ARHGEF6 encoding a guanine nucleotide exchange factor for Rho GTPases in patients with X-linked mental retardation Nat Genet 26:247–250.

Lamarche N, Hall A. 1994. GAPs for rho-related GTPases. Trends Genet 10:436–440.

Li HS, Chen JH, Wu W, Fagaly T, Zhou L, Yuan W, Dupuis S, Jiang ZH, Nash W, Gick C, Ornitz DM, Wu JY, Rao Y. 1999. Vertebrate slit, a secreted ligand for the transmembrane protein roundabout, is a repellent for olfactory bulb axons. Cell 96:807–818.

Matsuzaki H, Wang PH, Hu J, Rava R, Fu GK. 2009. High resolution discovery and confirmation of copy number variants in 90 Yoruba Nigerians. Genome Biol 10:R125.

Molinari F, Raas-Rothschild A, Rio M, Fiermonte G, Encha-Razavi F, Palmieri L, Palmieri F, Ben-Neriah Z, Kadhom N, Vekemans M, Attie-Bitach T, Munnich A, Rustin P, Colleaux L. 2005. Impaired mitochondrial glutamate transport in autosomal recessive neonatal myoclonic epilepsy. Am J Hum Genet 76:334–339.

Nannya Y, Sanada M, Nakazaki K, Hosoya N, Wang L, Hangaishi A, Kurokawa M, Chiba S, Bailey DK, Kennedy GC, Ogawa S. 2005. A robust algorithm for copy number detection using high-density oligonucleotide single nucleotide polymorphism genotyping arrays. Cancer Res 65: 6071–6079.

Ohtahara S, Yamatogi Y. 2006. Ohtahara syndrome: With special reference to its developmental aspects for differentiating from early myoclonic encephalopathy. Epilepsy Res 70:S58–S67.

Saitsu H, Kato M, Mizuguchi T, Hamada K, Osaka H, Tohyama J, Uruno K, Kumada S, Nishiyama K, Nishimura A, Okada I, Yoshimura Y, Hirai S, Kumada T, Hayasaka K, Fukuda A, Ogata K, Matsumoto N. 2008. De novo mutations in the gene encoding STXBP1 (MUNC18-1) cause early infantile epileptic encephalopathy. Nat Genet 40:782–788.

Stromme P, Mangelsdorf ME, Shaw MA, Lower KM, Lewis SM, Bruyere H, Lutcherath V, Gedeon AK, Wallace RH, Scheffer IE, Turner G, Partington M, Frints SG, Fryns JP, Sutherland GR, Mulley JC, Gecz J. 2002. Mutations in the human ortholog of Aristaless cause X-linked mental retardation and epilepsy. Nat Genet 30:441–445.

Tenoever BR, Ng SL, Chua MA, McWhirter SM, Garcia-Sastre A, Maniatis T. 2007. Multiple functions of the IKK-related kinase IKKepsilon in interferon-mediated antiviral immunity. Science 315:1274–1278.

Triglia T, Peterson MG, Kemp DJ. 1988. A procedure for in vitro amplification of DNA segments that lie outside the boundaries of known sequences. Nucleic Acids Res 16:8186.

Weaving LS, Christodoulou J, Williamson SL, Friend KL, McKenzie OL, Archer H, Evans J, Clarke A, Pelka GJ, Tam PP, Watson C, Lahooti H, Ellaway CJ, Bennetts B, Leonard H, Gecz J. 2004. Mutations of CDKL5 cause a severe neurodevelopmental disorder with infantile spasms and mental retardation. Am J Hum Genet 75:1079–1093.

Wong K, Ren XR, Huang YZ, Xie Y, Liu G, Saito H, Tang H, Wen L, Brady-Kalnay SM, Mei L, Wu JY, Xiong WC, Rao Y. 2001. Signal transduction in neuronal migration: Roles of GTPase activating proteins and the small GTPase Cdc42 in the Slit-Robo pathway. Cell 107:209–221.

Wu W, Wong K, Chen J, Jiang Z, Dupuis S, Wu JY, Rao Y. 1999. Directional guidance of neuronal migration in the olfactory system by the protein Slit. Nature 400:331–336.

Yao Q, Jin W-L, Wang Y, Ju G. 2008. Regulated shuttling of Slit-Robo-GTPase activating proteins between nucleus and cytoplasm during brain development. Cell Mol Neurobiol 28:205–221.

Published in final edited form as:
Am J Med Genet A. 2011 July ; 155(7): 1511–1516. doi:10.1002/ajmg.a.34074.

Spectrum of *MLL2* (*ALR*) mutations in 110 cases of Kabuki syndrome

Mark C. Hannibal[1,2,*], **Kati J. Buckingham**[1,*], **Sarah B. Ng**[3,*], **Jeffrey E. Ming**[4], **Anita E. Beck**[1,2], **Margaret J. McMillin**[2], **Heidi I. Gildersleeve**[1], **Abigail W. Bigham**[1], **Holly K. Tabor**[1,2], **Heather C. Mefford**[1,2], **Joseph Cook**[1], **Koh-ichiro Yoshiura**[5], **Tadashi Matsumoto**[5], **Naomichi Matsumoto**[6], **Noriko Miyake**[6], **Hidefumi Tonoki**[7], **Kenji Naritomi**[8], **Tadashi Kaname**[8], **Toshiro Nagai**[9], **Hirofumi Ohashi**[10], **Kenji Kurosawa**[11], **Jia-Wei Hou**[12], **Tohru Ohta**[13], **Deshung Liang**[14], **Akira Sudo**[15], **Colleen A. Morris**[16], **Siddharth Banka**[17], **Graeme C. Black**[17], **Jill Clayton-Smith**[17], **Deborah A. Nickerson**[3], **Elaine H. Zackai**[4], **Tamim H. Shaikh**[18], **Dian Donnai**[17], **Norio Niikawa**[13], **Jay Shendure**[3], and **Michael J. Bamshad**[1,2,3]

[1] Department of Pediatrics, University of Washington, Seattle, Washington, USA [2] Seattle Children's Hospital, Seattle, Washington, USA [3] Department of Genome Sciences, University of Washington, Seattle, Washington, USA [4] Department of Pediatrics, The Children's Hospital of Philadelphia, The University of Pennsylvania School of Medicine, Philadelphia, Pennsylvania, USA [5] Department of Human Genetics, Nagasaki University Graduate School of Biomedical Sciences, Nagasaki, Japan [6] Department of Human Genetics, Yokohama City University Graduate School of Medicine, Yokohama, Japan [7] Department of Pediatrics, Tenshi Hospital, Sapporo, Japan [8] Department of Medical Genetics, University of the Ryukyus, Okinawa, Japan [9] Department of Pediatrics, Dokkyo Medical University, Koshigaya Hospital, Saitama, Japan [10] Division of Medical Genetics, Saitama Children's Medical Center, Saitama, Japan [11] Division of Clinical Genetics, Kanagawa Children's Medical Center, Yokohama, Japan [12] Department of Pediatrics, Chang Gung Children's Hospital, Taoyuan, Taiwan, Republic of China [13] Research Institute of Personalized Health Sciences, Health Sciences University of Hokkaido, Hokkaido, Japan [14] National Laboratory of Medical Genetics, Xiangya Hospital, Central South University, Republic of China [15] Department of Pediatrics, Sapporo City General Hospital, Sapporo, Japan [16] University of Nevada School of Medicine, Las Vegas, Nevada, USA [17] Department of Genetic Medicine, Manchester Academic Health Sciences Centre, University of Manchester, England [18] Department of Pediatrics, University of Colorado, Denver, Colorado, USA

Abstract

Kabuki syndrome is a rare, multiple malformation disorder characterized by a distinctive facial appearance, cardiac anomalies, skeletal abnormalities, and mild to moderate intellectual disability. Simplex cases make up the vast majority of the reported cases with Kabuki syndrome, but parent-to-child transmission in more than a half-dozen instances indicates that it is an autosomal dominant disorder. We recently reported that Kabuki syndrome is caused by mutations in *MLL2*, a gene that encodes a Trithorax-group histone methyltransferase, a protein important in the epigenetic control of active chromatin states. Here, we report on the screening of 110 families with Kabuki syndrome. *MLL2* mutations were found in 81/110 (74%) of families. In simplex cases for which DNA was available from both parents, 25 mutations were confirmed to be *de novo*, while a transmitted *MLL2* mutation was found in two of three familial cases. The majority of variants found to cause Kabuki syndrome were novel nonsense or frameshift mutations that are predicted

Corresponding author: Mike Bamshad, MD, Department of Pediatrics, University of Washington School of Medicine, Box 356320, 1959 NE Pacific Street, Seattle, WA 98195, mbamshad@u.washington.edu, Phone: (206) 221-4131, Fax: (206) 221-3795.
*These authors contributed equally to this work.

to result in haploinsufficiency. The clinical characteristics of *MLL2* mutation-positive cases did not differ significantly from *MLL2* mutation-negative cases with the exception that renal anomalies were more common in *MLL2* mutation-positive cases. These results are important for understanding the phenotypic consequences of *MLL2* mutations for individuals and their families as well as for providing a basis for the identification of additional genes for Kabuki syndrome.

Keywords

Kabuki syndrome; *MLL2*; *ALR*; Trithorax group histone methyltransferase

INTRODUCTION

Kabuki syndrome (OMIM#147920) is a rare, multiple malformation disorder characterized by a distinctive facial appearance, cardiac anomalies, skeletal abnormalities, and mild to moderate intellectual disability. It was originally described by Niikawa et al. [1981] and Kuroki et al. [1981] in 1981, and to date, about 400 cases have been reported worldwide [Adam and Hudgins, 2005; Niikawa et al., 1988; White et al., 2004]. The spectrum of abnormalities found in individuals with Kabuki syndrome is diverse, yet virtually all affected persons are reported to have similar facial features consisting of elongated palpebral fissures, eversion of the lateral third of the lower eyelids, and broad, arched eyebrows with lateral sparseness. Additionally, affected individuals commonly have severe feeding problems, failure to thrive in infancy and height around or below the 3rd centile for age in about half of cases.

We recently reported that a majority of cases of Kabuki syndrome are caused by mutations in *mixed lineage leukemia 2* (*MLL2*; OMIM#602113), also known as either *MLL4* or *ALR* [Ng et al., 2010]. *MLL2* encodes a SET-domain-containing histone methyltransferase important in the epigenetic control of active chromatin states [FitzGerald and Diaz, 1999]. Exome sequencing revealed that nine of ten individuals had novel variants in *MLL2* that were predicted to be deleterious. A single individual had no mutation in the protein-coding exons of *MLL2*, though in retrospect, his phenotypic features are somewhat atypical of Kabuki syndrome. In a larger validation cohort screened by Sanger sequencing, we found *MLL2* mutations in approximately two-thirds of 43 Kabuki cases, suggesting that Kabuki syndrome is genetically heterogeneous.

Herein we report on the results of screening *MLL2* for mutations in 110 families with one or more individuals affected with Kabuki syndrome in order to: (1) characterize the spectrum of *MLL2* mutations that cause Kabuki syndrome; (2) determine whether *MLL2* genotype is predictive of phenotype; (3) assess whether the clinical characteristics of *MLL2* mutation-positive cases differ from *MLL2* mutation-negative cases; and (4) delineate the subset of Kabuki cases that are *MLL2* mutation-negative for further gene discovery studies.

MATERIALS AND METHODS

Subjects

Referral for inclusion into the study required a diagnosis of Kabuki syndrome made by a clinical geneticist. From these cases, phenotypic data were collected by review of medical records, phone interviews, and photographs. These data were summarized by each collaborating clinician and forwarded for review to two of the authors (MB and MH). These data were collected from five different clinical genetics centers in three different countries and over a protracted period of time and forwarded for review to two of the authors (MB and MH). Data on certain phenotypic characteristics including stature, feeding difficulties, and

failure to thrive was not uniformly collected or standardized. Therefore, we decided to be conservative in our analysis and use only phenotypic traits that could be represented by discrete variables (i.e., presence or absence) and for which data were available from at least 70% of cases. In addition, these clinical summaries were de-identified and therefore facial photographs were unavailable from most cases studied. Written consent was obtained for all participants who provided identifiable samples. The Institutional Review Boards of Seattle Children's Hospital and the University of Washington approved all studies. A summary of the clinical characteristics of 53 of these individuals diagnosed with Kabuki syndrome has been reported previously [Ng et al., 2010].

Mutation analysis

Genomic DNA was extracted using standard protocols. Each of the 54 exons of *MLL2* was amplified using Taq DNA polymerase (Invitrogen, Carlsbad, CA) following manufacturer's recommendations and using primers previously reported [Ng et al. 2010]. PCR products were purified by treatment with exonuclease I (New England Biolabs, Inc., Beverly, MA) and shrimp alkaline phosphatase (USB Corp., Cleveland, OH), and products were sequenced using the dideoxy terminator method on an automatic sequencer (ABI 3130xl). The electropherograms of both forward and reverse strands were manually reviewed using CodonCode Aligner (Dedham, MA). Primer sequences and conditions are listed in Supplementary Table I.

For *MLL2* mutation-negative samples, DNA was hybridized to commercially available whole-genome tiling arrays consisting of one million oligonucleotide probes with an average spacing of 2.6 kb throughout the genome (SurePrint G3 Human CGH Microarray 1×1M, Agilent Technologies, Santa Clara, CA). Twenty-one probes on this array covered *MLL2* specifically. Data were analyzed using Genomics Workbench software according to manufacturer's instructions.

RESULTS

All 54 protein-coding exons and intron-exon boundaries of *MLL2* were screened by Sanger sequencing in a cohort of 110 kindreds with Kabuki syndrome. This cohort included 107 simplex cases (including a pair of monozygotic twins) and three familial (i.e., parent-offspring) cases putatively diagnosed with Kabuki syndrome. Seventy novel *MLL2* variants that were inferred to be disease-causing were identified in 81/110 (74%) kindreds (Fig 1 and Supplementary Table II online). These eighty-one mutations included 37 nonsense mutations (32 different sites and five sites with recurrent mutations), three in-frame deletions or duplications (2 different sites and 1 site with a recurrent mutation), 22 frameshifts (22 different sites), 16 missense mutations (11 different sites and four sites with recurrent mutations) and 3 splice consensus site (or intron-exon boundary) mutations. None of these variants were found in dbSNP (build 132), the 1000 Genomes Project pilot data, 190 chromosomes from individuals matched for geographical ancestry. In total, pathogenic variants were found at seventy sites. Additionally, there were ten sites at which recurrent mutations were observed.

For 25 simplex cases in which we identified *MLL2* mutations, DNA was available from both unaffected parents, and in each case the mutation was confirmed to have arisen *de novo* (Supplementary Table II online). These included 14 nonsense, five frameshift, three missense, two splice site mutations and one deletion. *De novo* events were confirmed at six of the 10 sites where recurrent mutations were noted. In addition to the 81 kindreds in which we identified causal *MLL2* mutations, we found two *MLL2* variants in each of three simplex cases. In each case, neither *MLL2* mutation could unambiguously be defined as disease-causing (Supplementary Table II online). In one case, we found both a 21 bp in-frame

insertion in exon 39 and a 1 bp insertion in exon 46 predicted to cause a frameshift. However, the unaffected mother also carried the 21 bp insertion suggesting that this is a rare polymorphism, and that the 1 bp deletion is the pathogenic mutation responsible for Kabuki syndrome.

Apparent disease-causing variants were discovered in nearly half (i.e., 22/54) of all protein-coding exons of *MLL2* and in virtually every region known to encode a functional domain (Fig 1). However, the distribution of variants appeared non-random as 13 and 12 novel variants were identified in exons 48 and 39, respectively. These sites accounted for 25, or more than one-third, of all the novel *MLL2* variants and 31/81 mutations that cause Kabuki syndrome in our cohort. Eleven of the 12 pathogenic variants in exon 39 were nonsense mutations and occurred in regions that encode long polyglutamine tracts.

Four of the families studied herein had two individuals affected with Kabuki syndrome. A pair of monozygous twins with a c.15195G>A mutation were concordant for mild developmental delay, congenital heart disease, preauricular pits and palatal abnormalities, but discordant for hearing loss, and a central nervous system malformation. Concordance for mild developmental delay between an affected parent and child was observed in two families with *MLL2* mutations, one with a nonsense mutation, c.13579A>T, p.K4527X, and the other with a missense mutation, c.16391C>T, p.T5464M that was also found in a simplex case. No *MLL2* mutation was found in the remaining affected parent and child pair.

To examine the relationship between genotype and phenotype, we first compared the frequency of developmental delay, congenital heart disease, cleft lip and/or palate, and structural renal defects between *MLL2* mutation-positive vs. *MLL2* mutation-negative cases. No significant difference was observed between groups for three of these four phenotypes (Table I, a). However, renal anomalies were observed in 47% (31/66 cases) of *MLL2* mutation-positive cases compared to 14% (2/14 cases) of *MLL2* mutation-negative cases and this difference was statistically significant (χ=5.1, df=1, p=0.024). In 35 cases in two clinical cohorts for whom more complete phenotypic data were available, short stature was observed in 54% (14/26) of *MLL2* mutation-positive cases compared to 33% (3/19 cases) of *MLL2* mutation-negative cases. We also divided the *MLL2* mutation-positive cases into those with nonsense and frameshift mutations and those with missense mutations and compared the frequency of developmental delay, congenital heart disease, cleft lip and/or palate, and structural renal defects between groups. No significant differences were observed between groups (Table I, b).

In 26 independent cases of Kabuki syndrome, including one parent-offspring pair, no *MLL2* mutation was identified. Both persons in the mother-child pair had facial characteristics consistent with Kabuki syndrome (Fig 2), mild developmental delay, and no major malformations. The mother is of Cambodian ancestry and her daughter is of Cambodian and European American ancestry. In general, most of the *MLL2* mutation-negative Kabuki cases had facial characteristics (Fig 3) similar to those of the *MLL2* mutation-positive Kabuki cases, and a similar pattern of major malformations (Table I) with the exception of fewer renal abnormalities.

We screened the *MLL2* mutation-negative cases by aCGH for large deletions or duplications that encompassed *MLL2*. Abnormalities were found in four cases. In one case, a 1.87 kb deletion of chromosome 5 (hg18, chr5:175,493,803-177,361,744) that included *NSD1* and had breakpoints in flanking segmental duplications identical to the microdeletion commonly found in Sotos syndrome, was found. This suggests that this individual has Sotos syndrome, not Kabuki syndrome [Kurotaki et al., 2002]. A second case had a novel 977-kb deletion of chromosome 19q13 (hg18, chr19:61,365,420–62,342,064) encompassing 20 genes. The

majority of genes within the deleted region are zinc finger genes, some of which are known to be imprinted in both human and mouse. A third case had a complex translocation t(8;18)(q22;q21). Finally, a fourth case was found to have extra material for the entire chromosome 12. Average log2 ratio across chromosome 12 was 0.49, most likely representing mosaic aneuploidy of chromosome 12. No aCGH abnormalities were observed in 21 cases and aCGH failed for one case.

DISCUSSION

We have expanded the spectrum of mutations in *MLL2* that cause Kabuki syndrome and explored the relationship between *MLL2* genotype and some of the major, objective phenotypic characteristics of Kabuki syndrome. The majority of variants found to cause Kabuki syndrome are either novel nonsense or frameshift mutations, and appear to arise *de novo*. While mutations that cause Kabuki syndrome are found throughout the *MLL2* gene, there appear to be at least two exons (39 and 48) in which mutations are identified with a considerably higher frequency. Mutations in these three exons account for nearly half of all mutations found in *MLL2*, while the length of these exons represents ~35% of the *MLL2* open reading frame (ORF). Furthermore, exon 48, the exon in which mutations are most common, comprises only ~7% of the *MLL2* ORF. Exon 39 contains several regions that encode long polyglutamine tracts suggesting the presence of a mutational hotspot, although no such explanation is obvious for exon 48. A stepwise approach in which these regions are the first screened might be a reasonable approach to diagnostic testing. However, capture of all introns, exons, and nearby *MLL2* regulatory regions followed by next-generation sequencing would be more comprehensive and likely to be less costly over the long term.

Comparison of four of the objective clinical characteristics of *MLL2* mutation-negative versus *MLL2* mutation-positive cases allowed us to explore both the relationship between *MLL2* genotype and Kabuki phenotype and the phenotype of *MLL2* mutation-negative cases. Overall, the clinical characteristics of *MLL2* mutation-positive cases did not differ significantly from *MLL2* mutation-negative cases with the exception that renal anomalies were more common in *MLL2* mutation-positive cases. Similarly, we observed no significant phenotypic—including the severity of developmental delay—differences between individuals grouped by mutation type. However, the phenotypic data available to us for analysis was limited and, for many cases, we lacked specific information about each malformation present. Furthermore, the most typical phenotypic characteristic, the distinctive facial appearance, was not compared in detail between cases although it would be of interest to study facial images 'blinded' to mutation status to investigate its power to predict genotype. Analysis of genotype-phenotype relationships using both a larger set of Kabuki cases, and with access to more comprehensive phenotypic information would be valuable.

No *MLL2* mutation could be identified in 26 of the cases referred to us with a diagnosis of Kabuki syndrome. In three of these cases, aCGH identified structural variants that could be of clinical significance although additional investigation is required. A fourth case had the classical deletion observed in individuals with Sotos syndrome, and in retrospect it appears that this case was included in the cohort erroneously. The 22 remaining cases, including one parent-offspring pair, represent individuals with fairly classic phenotypic features of Kabuki syndrome without a *MLL2* mutation. This observation suggests that Kabuki syndrome is genetically heterogeneous. To this end, in these 22 cases, we sequenced the protein-coding exons of *UTX*, a gene that encodes a protein that directly interacts with *MLL2* but no pathogenic changes were found (data not shown). Exome sequencing of a subset of these *MLL2* mutation-negative cases to identify other candidate genes for Kabuki syndrome is underway.